

Design and Development of a Solar-Powered Rotary Drum Composter for Managing Food-Waste at the University Food Center

Ma. Angelica B. Danga¹, John Kevin C. Lim², Jude Milbert C. Jingco³, Justine Roi P. Manalo⁴, Joshua G. Marquez⁵, Alma L. Tanguangco⁶, Genesis M. Tiria⁷, Jezeth Vince B. Macaspac⁸

^[1-8] Don Honorio Ventura State University
Villa De Bacolor, Pampanga, Philippines
^[1]Email: 2020100950 [AT] dhvsu.edu.ph

ABSTRACT— *The annual value of food waste generated worldwide already reached a staggering \$1 trillion. This amounts to 1.3 – 1.4 billion tonnes or one third of food produced for human consumption that goes to waste each year. The Food Center at Don Honorio Ventura State University faces a similar issue a weekly production of 21.5kg of food waste. To address this increasingly concerning issue, a solar-powered rotary drum composter driven by a DC motor was developed. This composter, designed to accommodate up to 20kg of food waste. Analysis of the composter's motor performance reveals significant relationships between voltage, current, speed, torque, efficiency and load. The voltage exhibits an inverse proportional relationship with load, steadily decreasing from 24.8V to 23.3V as the load increases, while the current shows a direct proportional relationship, consistently rising from 4.1A to 9.84A with increased load. Further examination of torque and speed in relation to load indicates a direct and inverse proportional relationship, respectively. Torque increases from 6.68Nm to 27.23Nm with increasing load, meanwhile, speed decreased from 72.74rpm to 55.16rpm. As for the efficiency, it was found out that the composter operates most efficiently when the drum is loaded 12kg, beyond which efficiency gradually declines with increasing load up to 20kg. This decline signifies the diminishing returns associated with higher loads, highlighting the importance of load optimization for sustained efficiency in composter operation.*

Keywords— Food Waste, Solar, Rotary Drum, Voltage, Current

1. INTRODUCTION

The annual value of food waste generated worldwide already reached a staggering \$1 trillion [1]. This amounts to 1.3 – 1.4 billion tonnes or one third of food produced for human consumption that goes to waste each year [2]. Out of this food wasted each year, around 13 percent are wasted between harvest and retail stages, and others are wasted at the consumer levels. The global food production of estimated 17 percent becomes waste in households, food service, and retail combined [2,3]. These numbers are at risk of further escalation due to the growth in the global economy and population [4], with projections indicating a potential increase to as much as 2.6 billion tonnes by 2025 [5]. If food waste were a nation, it would rank as the third-largest contributor to greenhouse gas emissions, trailing only China and the United States [6]. Of the total annual food waste production, a significant portion, amounting to 275 million tonnes, is accounted for in South and Southeast Asia, where Philippines is a part of [3].

This worldwide concern regarding food waste is similarly evident in the country, which if not addressed could result in compounding challenges. In 2016, the typical Filipino family generates 66.8g of plate waste each day which is 5.0g more than in 2015, where it was disclosed that among typical plate waste, cereals and cereal products constituted 48.0g, while fish, meat, and poultry accounted for 8.9g. Additionally, 7.2g comprised vegetables, leaving the remaining 2.7g to represent various other food categories [7, 8].

Table 1: University Food Center's Generated Waste for 5 days

5 Days Collection and Amount of Collected Waste in kg (September 25-29, 2023)						
Type of Waste	Monday	Tuesday	Wednesday	Thursday	Friday	Total
Paper Cups	1.5	2	1.8	2.2	1.3	8.8
PET Bottles	4	3.75	2.5	2	2.8	15.05
Plastic Wrappers	1	0.6	0.75	0.5	0.5	3.35
Food Waste	5	5	4.25	3.75	3.5	21.5
Residual	14.5	8.8	9	13.4	11	56.7

2. METHODS

In order to accomplish a successful research project leading to the development of a solar-powered composter, data on the UFC's five-day generated waste was collected and categorized by waste type. From this data, the volume input of food waste to the composter is considered for the specification of the composter. Then, the materials and electrical components that are needed to develop the composter are identified.

In addition, according to [15], the most optimum mixture of organic waste for composting in a rotating drum is a food waste to bulking agent mass ratio of 1:0.5. This ratio of organic waste achieves better result regarding waste reduction volume, which is seen as a positive feature as more waste could be treated. Moreover, if available it is also recommended to add animal manure, at least 10% of the volume of the food waste for more degradation of organic matter. In case the compost emits strong foul odour, addition of charcoal reduces this.

2.1 Solar-Powered Rotary Drum Components

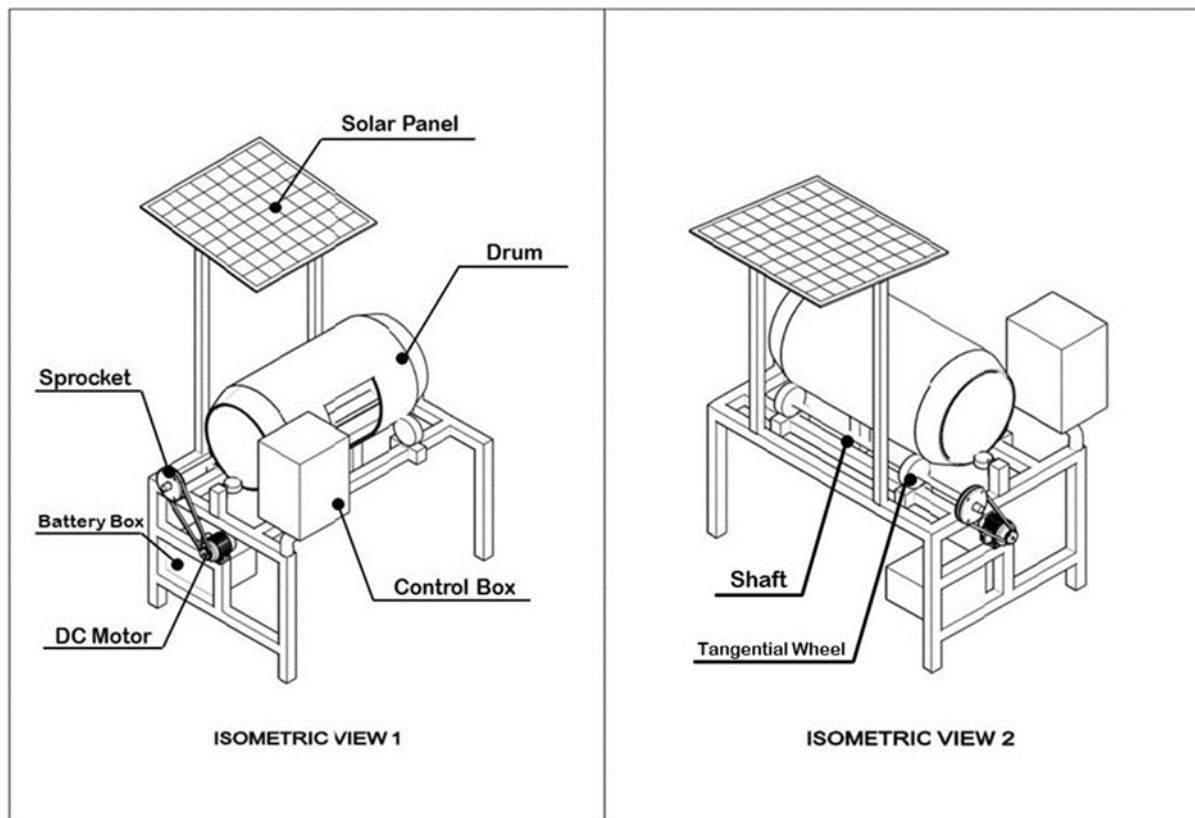


Figure 1: Frame Design of a Solar-Powered Rotary Composter

The solar-powered rotary drum comprises several key components that facilitate its operation. These components are categorised into two main groups: the rotating mechanism and the electrical components. The rotating mechanism includes the drum, DC motor, and sprocket, all working in tandem to drive the motion of the drum. On the other hand, the electrical components consist of a battery, solar panels, control box, and necessary wiring with overcurrent protection devices. Together, these components form a cohesive system, harnessing solar energy to power the rotary drum.

2.2 Rotating Mechanism

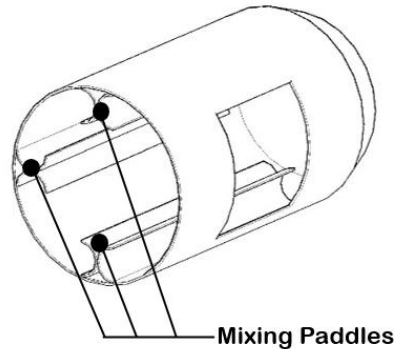


Figure 2: Drum Design

Drum: Formula (1) is used to determine the minimum volume of the drum with the weight and density of the input food waste considered which is at maximum of 20kg, and 290 kg/m³ [3] respectively. Therefore, a 170L PVC drum was used. Moreover, there will be a 50% [16] allowance to the drum's volume for opening the drum during loading.

$$\text{Volume of drum} = \frac{\text{Full capacity of drum in kg}}{\text{density of food waste}} \times 150\% \quad (1)$$

To guarantee thorough mixing of the compost, three sets of mixing paddles crafted from PVC tubes, 29 inches in length and 5 inches in width were riveted onto the drum's walls, positioned approximately 90 degrees apart from each other.

DC Motor: The motor that will drive the system was determined by formula (2) whereas it depends on the predetermined speed of the rotary, torque requirement to rotate the drum at its full load, and the 1.5 safety factor of dc motor [19]. Hence, a 250W Motor with nameplate values of 24VDC, 330 rpm, 13A full load current was used.

$$P_M = \frac{2\pi NT}{60} \times 1.5 \quad (2)$$

Sprocket: To meet the necessary speed and torque requirement to drive the drum, a reduction gear will be used to connect the motor and the shaft of the axel that will rotate the drum, the reduction ratio is dependent on the ratio of the rated speed of the motor under normal conditions and the rotational speed of the drum (3). The motor has a rated speed of 330 rpm and must be reduced to at least 10rpm, recommended in [15,16,17]. Hence, a gear reduction ratio of at least 33:1.

$$G.R. = \frac{N_1}{N_2} = \frac{T_2}{T_1} \quad (3)$$

2.3 Electrical Components

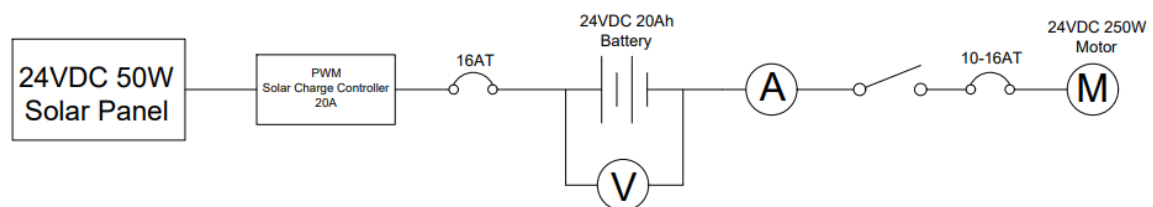


Figure 3: Single-Line Diagram

The electrical system that supplies power to the 24V DC motor are composed of two 12V 25W solar panel connected in series, two 12V 20ah lead-acid battery in series is in charge to make sure that the system can autonomously run at least for four days, and a solar charge controller which will regulate the current in charging the battery.

Battery Bank: As shown in formula (4), when selecting the power bank, four key factors were considered: the chosen system voltage, total demand energy (T.D.E.), days of autonomy (D.o.A.), and depth of discharge (D.o.D.). A 24V system was used due to the motor's nominal voltage requirement. T.D.E. was calculated based on the motor's power rating, daily operating hours, and the cumulative percent loss across system components. Additionally, a four-day autonomy period and a 50% depth of discharge were established, given the utilization of a lead-acid battery [20].

$$\text{Battery Bank Capacity (Ah)} = \frac{(T.D.E.)(D.o.A.)}{(D.o.D.)(24V)} \quad (4)$$

$$T.D.E. = (P_m)(\text{Operating Hours per day})(1 + \sum \% \text{loss of the system components}) \quad (5)$$

Solar Panel Rating: For a 24V system, the minimum solar panel rating required to charge the battery can be calculated using formula (6). This rating is influenced by factors such as the capacity of the battery bank (set at 20Ah), the D.o.D. of the battery, and the peak sun hours [20], which in the Philippines ranges from 4.5 to 5 hours [21].

$$\text{Solar Panel Rating} = \frac{(24V)(\text{Battery Bank Capacity})(D.o.D.)}{\text{Peak sun hours}} \quad (6)$$

Solar Charge Controller: The minimum rating for the solar charge controller was determined by multiplying a 125% safety factor to the short-circuit current rating I_{SC} of the PV module and the number of PV modules in parallel connection (7). Since the I_{SC} rating of a 12V 25W module was 1.49A, and there was only one string of PV modules connected in series, the minimum rating of the solar charge controller to be use should be 1.86A. However, as there was no solar charge controller with this specific rating, the next higher available rating, which was 20A, was chosen for use.

$$\text{SCC rating} = (1.25)(I_{SC})(\text{No. of PV module in parallel}) \quad (7)$$

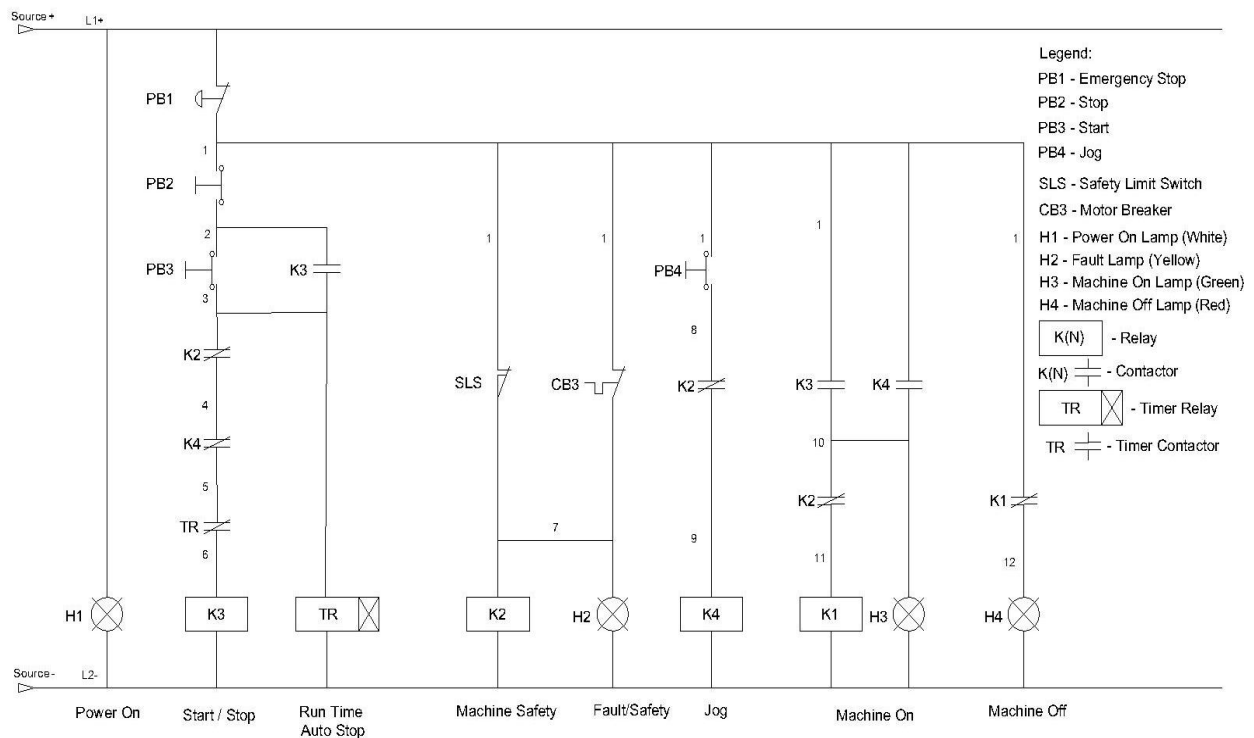


Figure 4: Control System Schematic Diagram

Control Panel: The control system for the motor is equipped with four buttons, namely PB1, PB2, PB3, and PB4. PB1, designated as the emergency stop, brings the machine to a halt in the event of an emergency or unsafe conditions. This button initiates a rapid shutdown process, cutting off power to all essential components to ensure a swift and effective response to potential hazards, prioritizing the safety of both the machine and its operators. Distinguished by a mushroom-shaped head and a prominent red color, PB1 is easily accessible for quick identification. In contrast, PB2 serves the stop button, being a more general control within the regular interface, facilitating routine halting of the machinery for planned activities or maintenance.

PB3 serves as the start button of the machine, activating its operation. Upon pressing PB3, it energizes the K3 relay, leading to the closure of the K3 contactor, contactor that is connected to the motor, and the initiation of current flow. This current, in turn, triggers a multifunction timer relay TR which has been integrated to restrict the machine's operation to the necessary duration for compost mixing, set with an on-delay feature and linked to a normally closed contactor coil. The machine continues its operation until the contactor coil opens at the predetermined time set for the relay. This methodical sequence ensures a controlled and timed operation of the machine. Meanwhile, PB4 functions as the jog button, acting as a control mechanism that allows operators to manually and momentarily move the drum. This feature was added so that when the drum's position makes it inconvenient for operators to load food waste, enabling precise adjustments during such scenarios.

This machine also features four LED lamp indicators: H1, H2, H3, and H4. H1 (White LED) signifies the availability of power for the machine. H2 (Yellow LED) signals a system fault, indicating that either the SLS is inactive or CB3 is open or tripped. H3 (Green LED) illuminates when the machine is powered on and operational, while H4 (Red LED) indicates available power but signifies that the machine is currently not in operation. Lastly, a digital meter for voltage and current has been incorporated into the control panel to oversee the motor's voltage and current levels.

Wires & Overcurrent Protection Devices: Wires and overcurrent protection are sized based on Philippine Electrical Code 2017 edition; article 6.90-Solar Photovoltaic (PV) Systems, article 6.92-Fuel Cell Systems, article 7.6-Energy Storage Systems, and article 4.30-Motors, Motor Circuits, and Controllers. The conductor size is calculated by PV modules to SCC, and from SCC to battery & load (DC Motor and Control Box), each with corresponding overcurrent protective devices.

To determine the appropriate wire size between the PV module and SCC, the maximum current I_{max} must be determined first. Section 6.90.2.2.(A)(1) of PEC states that in order to calculate for the I_{max} of the PV system, the I_{SC} of each PV module connected in parallel must be added and multiplied by 125 percent (8) which yields a 1.86A of I_{max} [22].

$$I_{max} = (\sum \text{Parallel - connected PV module rated } I_{SC}) \times 125\% \quad (8)$$

Equation (8) then establishes the basis for sizing the PV module to SCC conductor $I_{PV \text{ Conductor}}$, in accordance with section 6.90.2.2.(B)(1), $I_{PV \text{ Conductor}}$ is equals to 125 percent of the I_{max} which results to an $I_{PV \text{ Conductor}}$ of 2.33A. The wire ampacity to be used in between the PV module and SCC shall then be greater than 2.33A. Therefore, 2.0mm² THHN Cu wire of 25A ampacity was used as PV conductors. [22].

$$I_{PV \text{ Conductor}} = I_{max} \times 125\% \quad (9)$$

Based on section 6.90.2.3. (A)(2), no overcurrent device is necessary for PV modules or PV source circuits if the total I_{SC} from all sources does not surpass the ampacity of the conductors and is in accordance with the maximum overcurrent protective device size rating specified for the PV module [22]. The nameplate I_{sc} , and maximum overcurrent protection rating is 1.49A, and 16AT respectively. Thus, as per the cited section, no overcurrent protection device is employed between the PV module and SCC.

Next, in determining the circuit conductor used for SCC to battery & load, whichever yields a greater current rating between formula 10 and section 7.6.2.4. is abided. The total current I_{total} supplied to the load is the summation of the motor control current $I_{motor \text{ control}}$ and the motor's rated full load current $Motor_{FLA}$ multiplied by the safety factor of 125% (10). In light with this, formula (10) requires a wire ampacity greater than 22.35A. On the other hand, according to section 7.6.2.4 [22], if a charge controller is installed, the ampacity of the conductors in output circuit shall be based on the maximum rated continuous output current of the charge controller for the selected output voltage range. Hence, the wire ampacity shall be greater than the SCC's maximum rated continuous output current of 20A. For this reason, the wire size used from SCC to battery & load is based of formula (10). As a result, 2.0mm² THHN Cu wire with a 25A ampacity was also utilized from SCC to battery & load [22].

$$I_{feeders} = I_{motor \text{ control}} + Motor_{FLA} \times 125\% \quad (10)$$

The overcurrent protection device which serves as the main breaker to separate the SCC and loads was also based of formula 10, and the resulting wire to be used. Hence, 20AT circuit breaker rating was used for the main breaker.

The size of wire that will feed current to the motor was calculated in accordance to section 4.30.2.3.(B)[22], where the ampacity of the conductor shall not be less than 125% of the nameplate current rating for a varying duty motor (11). Therefore, 2.0mm² THHN Cu wire of 25A ampacity was also used since (11) yields 16.75A.

$$I_{motor} = Motor_{FLA} \times 125\% \quad (11)$$

Meanwhile, an adjustable instantaneous trip circuit breaker ranging from 10T- 16AT was used for the motor branch-circuit short-circuit and ground-fault protection since according to section 4.30.4.2.(B), among other short-circuit and ground-fault protection devices, an adjustable instantaneous trip circuit breaker also known as motor-circuit protectors is allowed to be used as long as the setting is only adjustable/adjusted to no more than 250% of the full-load current of the motor [22].

The conductors employed in the motor control circuit, connecting various controller components such as timers, relays, and LED lights, used 0.75mm² Cu wire. This wire gauge was chosen because the motor control, during its initial testing, drew a current of less than 1A. As for the overcurrent protection device, Section 4.30.6.2.(B)(1)[22] stipulates that if the motor's overcurrent protective device fails to offer protection to the motor control circuit, a separate safeguard must be implemented. Importantly, this additional overcurrent protection should not exceed 7A for 0.75mm² Cu wire. Hence, 4AT rating of overcurrent protection was used.

2.4 Data Gathering & Data Treatment

In gathering the data needed for the objective, the machine was tested by loading the machine in increments of 4kg from 0kg to 20kg. Next, the following parameters were measured at each load increment of 4kg: voltage, current, speed, and continuous output torque. Voltage and current was measured using a digital and analogue voltage and current meter, speed in rpm was measured through a tachometer, and to measure the continuous output torque, a torque sensor coupled with a dynamometer to vary the load was used.

The mass of the compost was used as the primary indicator whether it was already fully decomposed or not, where the compost must have reduced its mass to 2kg per 4kg of food waste input as an indication that it is already decomposed fully. Moreover, physical appearance wise it should appear dark color similar to rich soil, its texture must be crumbly, but not sticky, and smells earthy.

Moreover, in determining the efficiency of the motor at each load. The mechanical output was calculated by multiplying the speed ω of drum (in rad/s), and the continuous output torque T (in Nm) of the motor (13).

$$P_{out} = T\omega = \frac{2\pi NT}{60} \quad (13)$$

And in determining the electrical input at each load on the other hand, the average voltage was multiplied with the average current (14).

$$P_{in} = V_{av}I_{av} \quad (14)$$

Thereafter, the mechanical output of the motor per load increment was divided by the electrical input per load increment and multiplied to 100 percent (15).

$$\eta_{@nth\ load} = \frac{P_{in}}{P_{out}} \times 100\% \quad (15)$$

3. RESULTS AND DISCUSSION

The main title (on the first page) should be centered, and in Times New Roman 18-point, boldface type. Capitalize the first letter of nouns, pronouns, verbs, adjectives, and adverbs; do not capitalize articles, coordinate conjunctions, or prepositions (unless the title begins with such a word). Please initially capitalize only the first word in (for example, "Format for Preparation of Paper for Publication in the AJCIS" — as in these guidelines).

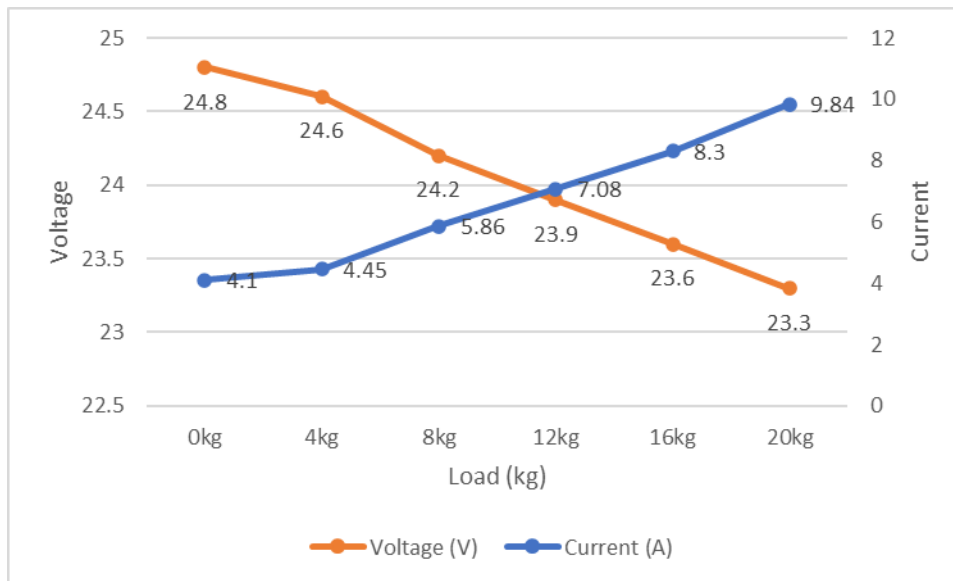


Figure 5: Voltage and Current at Different Loads

Figure 5 shows the variation of voltage and current across and through the motor when it is under load of 0kg, 4kg, 8kg, 12kg, 16kg, and 20kg. It is evident from the figure that the voltage has inverse proportional relationship with load since the voltage continuously dropped from 24.8V to 23.3V as the load inside the drum was increased from 0kg to 20kg. Meanwhile, the current has a direct proportional relationship with load where the current consistently increased from 4.1A to 9.84A when the load was also increased from 0kg to 20kg. This increase in current in respect to increase in load is due to the motor requiring more torque to overcome the resistance and maintain its speed. To produce more torque, the motor draws more current from the power source to generate a stronger magnetic field. On the other hand, due to this increase in current, the voltage also drops respectively. Since as the current increases the voltage drop across the internal resistance of the battery also increases therefore affecting the terminal voltage of the battery which is also the applied voltage across the motor terminals [18, 23]. This vary in voltage is however acceptable according to the National Electrical Manufacturers Association (NEMA), whereas according to NEMA MG1-2016 Section 12.44.1, motors are electrically designed around the expected supply voltage with a tolerance of +/- 10% voltage-maximum for small- and medium-voltage electric motors.

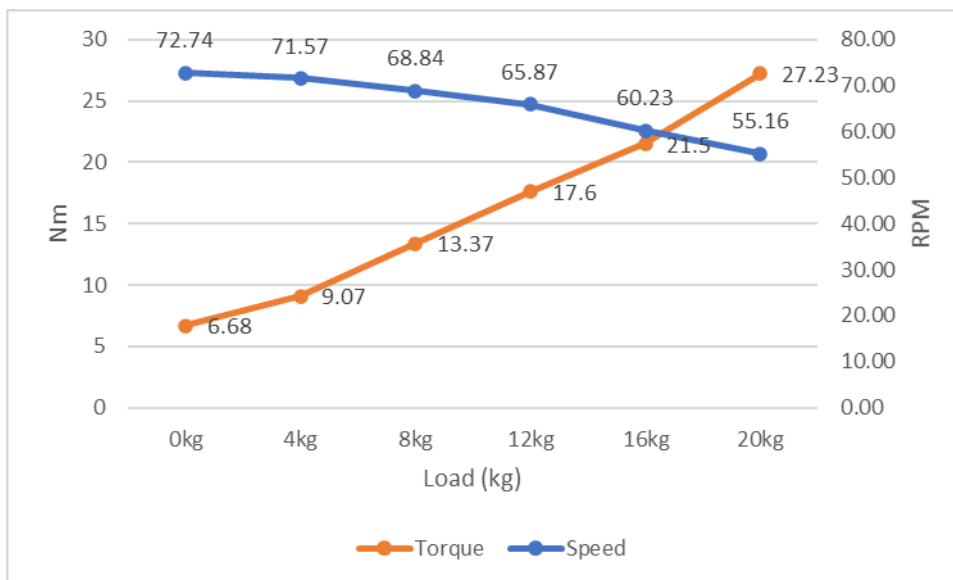


Figure 6: Speed and Torque at Different Loads

Figure 6 shows the variation of continuous output torque and speed of the motor when it is under load of 0kg, 4kg, 8kg, 12kg, 16kg, and 20kg. Drawing relationship between torque and speed to the load, it can be said that the torque, and the speed of the motor has a direct, and inverse proportional relationship against its load. To be specific, the torque of the motor increased from 6.68Nm to 27.23Nm as the load increased from 0kg to 20kg. This increase in torque arises to overcome the load and maintain its rotational motion. On the other hand, as the load increases, the motor slows down

from 72.4rpm to 55.16rpm, which according to [18, 23] is due to the back EMF being reduced which in turn allows more current to flow through the windings to maintain torque. However, this increase in current results in a larger voltage drop across the internal resistance of the motor, further reducing the effective voltage available for driving the motor.

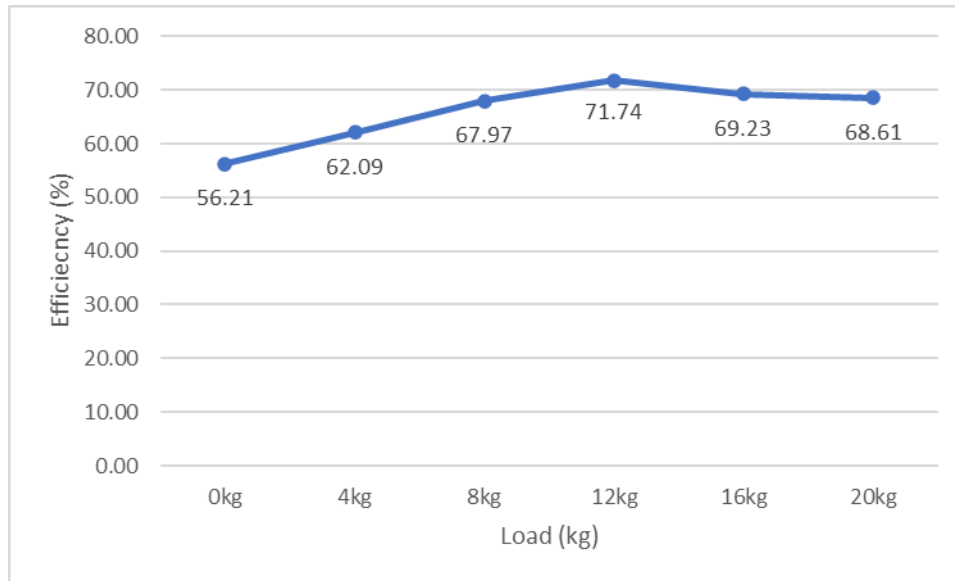


Figure 7: Efficiency of the Motor

Figure 7 shows the efficiency of the motor relative to the load of the drum. It can be seen that the efficiency continues to increase along with the load until it was loaded up to 12kg, where it can be said that the motor operates most efficiently at this point. After this maximum efficiency point, the efficiency starts to decline as the load continued to increase up to 20kg.

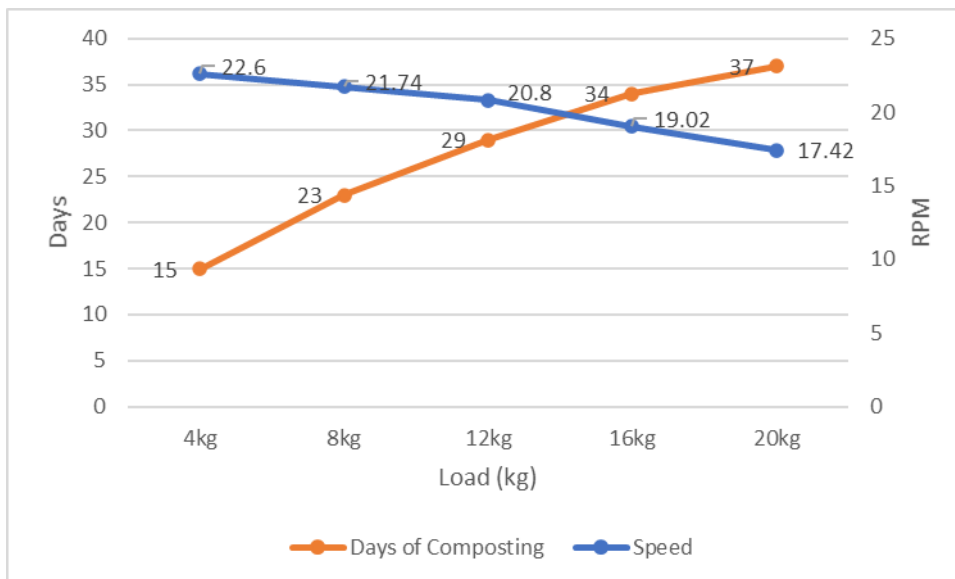


Figure 8: Days of Composting and Rotational Speed

Figure 8 shows the relation between the speed of the drum with the duration of composting at different loads. For instance, at a rotation speed of 22.6 rpm, the food waste is converted to compost in 15 days. When the speed is reduced to 21.74 rpm, it takes 23 days, at 20.8 rpm, it takes 29 days, at 19.02 rpm, it takes 34 days, and at 17.42 rpm, it takes 37 days.

4. CONCLUSION AND RECOMMENDATION

In conclusion, the experimental analysis of the motor under varying loads reveals several significant relationships between voltage, current, torque, speed, and efficiency. The voltage exhibits an inverse proportional relationship with load, steadily decreasing as the load increases, while the current shows a direct proportional relationship, consistently rising with increased load. This phenomenon occurs as the motor demands more torque to overcome resistance and

maintain its rotational speed, leading to an increase in current draw from the power source. Consequently, the voltage drop across the internal resistance of the battery affects the terminal voltage applied across the motor terminals, in line with NEMA standards.

The torque and speed exhibit a direct and inverse proportional relationship with the load, respectively. As the load increases, the torque rises to overcome it while the speed decreases due to a reduction in back EMF, allowing more current to flow through the windings to maintain torque. However, this increase in current also results in a larger voltage drop across the motor's internal resistance, further diminishing the effective voltage available for driving the motor, hence slowing down the motor.

Moreover, efficiency initially increases with the load until reaching a peak efficiency point at 12kg. Beyond this optimal load, efficiency begins to decline as the load continues to increase up to 20kg. This trend is expected as the motor operates most efficiently when its load matches its design parameters, and deviations from this optimal point led to decreased efficiency. Meanwhile, the days of composting increases as the mass of food waste increases. However, the days of composting of for every increment decrease compared to each previous increment.

Further studies might explore the capability of this machine by implementing an effective battery management strategy through a voltage regulator to optimize the balance between discharging (motor operation) and charging (solar panel utilization) to maintain constant voltage all throughout. One might explore opportunities to fine-tune measurement instruments to enhance the precision of quantifications. It is also possible to develop system integration and control algorithms to optimize the coordination between the motor, energy storage, and solar panel components. This includes predictive control strategies, dynamic load management, and adaptive power management algorithms.

5. REFERENCES

- [1] Food and Agriculture Organization of the United Nations. Key facts on food loss and waste you should know! <http://www.fao.org/save-food/resources/keyfindings/en/>. (accessed October 18, 2023).
- [2] FAO, WFP, IFAD, UNICEF W. (2017). The state of food security and nutrition in the world. Building resilience for peace and food security. Int J Phytore- mediation. Available from: <https://www.fao.org/3/I7695e/I7695e.pdf>.
- [3] "Food loss and waste reduction". United Nations. <https://www.un.org/en/observances/end-food-waste-day> (accessed Oct. 18, 2023).
- [4] Ebikade, Elvis, et al. (2020). "The future is garbage: repurposing of food waste to an integrated biorefinery." ACS Sustainable Chemistry & Engineering 8.22: 8124-8136.
- [5] Kumar, Vinay, et al. (2022). "Emerging challenges for the agro-industrial food waste utilization: A review on food waste biorefinery." Bioresource Technology: 127790.
- [6] U.S. Energy Information Administration. U.S. energy facts explained - consumption and production - U.S. Energy Information Administration (EIA) <https://www.eia.gov/energyexplained/us-energy-facts/> (accessed October 18, 2023).
- [7] Department of Health, Department of Social Welfare and Development. Environmental and Social Management Framework The Philippine Multi-sectoral Nutrition Project. (2022). <https://kalahi.dswd.gov.ph/phocadownload/Philippine%20Multisectoral%20Nutrition%20Project%20-%20Env%20ironmental%20and%20Social%20Management%20Framework,%2011Feb2022.pdf>. (Accessed 18 Oct 2023).
- [8] Department of Science and Technology – Food and Nutrition Research Institute (DOST-FNRI). (2022). Consumption Survey. <http://enutrition.fnri.dost.gov.ph/site/uploads/2018-2019%20Facts%20and%20Figures%20-%20Food%20Consumption%20Survey.pdf>. (Accessed 18 October 2023).
- [9] Anh, L. H., Thanh Truc, N. T., Tuyen, N. T. K., et al. (2021). Site-specific determination of methane generation potential and estimation of landfill gas emissions from municipal solid waste landfill: a case study in Nam Binh Duong, Vietnam. *Biomass Conversion and Biorefinery*, 1-12.
- [10] Lv, Yuanyuan, et al. (2021). "Anaerobic co-digestion of food waste with municipal solid waste leachate: A review and prospective application with more benefits." *Resources, Conservation and Recycling* 174.
- [11] Wang, Yumei, et al. (2021). "Aeration rate improves the compost quality of food waste and promotes the decomposition of toxic materials in leachate by changing the bacterial community." *Bioresource Technology* 340.
- [12] Kalamdhad, A. S., & Kazmi, A. A. (2009). Effects of turning frequency on compost stability and some chemical characteristics in a rotary drum composter. *Chemosphere*, 74(10), 1327-1334.
- [13] Peng, Lijuan, et al. "Effect of aeration rate, aeration pattern, and turning frequency on maturity and gaseous emissions during kitchen waste composting." *Environmental Technology & Innovation* 29 (2023): 102997.
- [14] Tang, Ruolan, et al. "Effect of moisture content, aeration rate, and C/N on maturity and gaseous emissions during kitchen waste rapid composting." *Journal of Environmental Management* 326 (2023): 116662.

- [15]T. Sayara, M. Shadouf, H. Issa, H. Obaid, and R. Hanoun, (2022). “Home composting of food wastes using rotary drum reactor as an alternative treatment option for organic household wastes.” *Journal of Ecological Engineering*. vol. 23, no. 6, pp. 139–147. doi:10.12911/22998993/147873.
- [16]Siti, F. Z., et al. (2021, November). Autonomous Solar Rotary Composter Equipped with a Remote Management System. In 2021 9th International Renewable and Sustainable Energy Conference (IRSEC) (pp. 1-5). IEEE.
- [17] M. M. Lahmadi et al. (2022). “New ecological composter powered by solar panels without battery to produce organic fertilizers,” *International Journal of Emerging Technology and Advanced Engineering*. vol. 12, no. 9, pp. 14–22. doi:10.46338/ijetae0922_02
- [18]Charles Seymour Siskind, *Electrical Machines*. McGraw-Hill/Glencoe, 1959.
- [19]Sayara, Tahseen, et al. (2020). "Recycling of organic wastes through composting: Process performance and compost application in agriculture." *Agronomy* 10.11: 1838.
- [20]Ejiko, S. O., & Olaniyi, D. (2018). Development of Regression Models for Appropriate Battery Banking Determination in Solar Power System. *IOSR Journal of Electrical and Electronics Engineering (IOSR-JEEE)*, 13(1), 30-37.
- [21]S. Ahmed, “Unlocking Rooftop Solar in the Philippines Energy-Supply Security and Lower Electricity Costs Energy Finance Analyst Unlocking Rooftop Solar in the Philippines,” 2018. Available: https://ieefa.org/wp-content/uploads/2018/08/IEEFA_Unlocking-Rooftop-Solar-in-the-Philippines_August-2018.pdf
- [22]Philippine Electrical Code, 2017th ed. (2017). Institute of Integrated Electrical Engineers.
- [23]Mehta, V. K., Mehta, R. (2002). *Principles of Electrical Machines*. India: S Chand & Company Limited.